ICES Journal of Marine Science, 2025, Vol. 0, Issue 0, fsaf138
https://doi.org/10.1093/icesjms/fsaf138
Received: 18 March 2025; **revised:** 2 July 2025; **accepted:** 22 July 2025
Original Article

Assessing red hind (*Epinephelus guttatus*) spawning aggregation changes from long-term relative variations in call types associated with reproductive behaviors

Laurent. M. Chérubin [1,*], Caroline Woodward [1], Michelle Schärer-Umpierre [2], Richard S. Nemeth [3], Richard Appeldoorn [4], Eric Appeldoorn-Sanders [4], Evan Tuohy [4], Ali K. Ibrahim [5]

[1]Harbor Branch Oceanographic Institute, Florida Atlantic University, FL, USA
[2]HJR Reefscaping, Boquerón, Puerto Rico
[3]Center for Marine and Environmental Studies, University of the Virgin Islands, Virgin Islands of the United States
[4]Department of Marine Sciences, University of Puerto Rico, Mayagüez Campus, Puerto Rico
[5]Department of Electrical Engineering and Computer Science (EECS), Florida Atlantic University, Boca Raton, FL, USA
*Corresponding author. Harbor branch Oceanographic Institute, Florida Atlantic University, FL, USA. E-mail: lcherubin@fau.edu

Abstract

Fish spawning aggregations (FSAs) are elevated concentrations of conspecific fish, often predictable in time and space, that gather for the main purpose of reproduction. For some grouper species, distinct courtship sounds are associated with specific reproductive behaviors, and this association has yet to be elucidated. If known, long-term trends in courtship sounds can thus be used as indicators of change in spawning aggregations. Red hind (*Epinephelus guttatus*) form spawning aggregations annually at recurring locations and times. Red hind have the ability to produce four distinct types of sounds (labeled RH1–4) that are most commonly heard during FSAs. Of these courtship-associated sounds (CAS), mostly two, produced by males, are used during courtship displays toward gravid females (RH1) and territorial/harem defense with other males (RH2), respectively. To elucidate the role of these two CAS in the red hind reproductive behaviors we analyzed the evolution of the partitioning between RH1 and RH2 call types in acoustic recordings spanning 12 years of spawning seasons, between 2011 and 2022 at a Caribbean FSA, off western Puerto-Rico. The relative temporal variations of call types were linked to the dynamics of the spawning population and suggests that daily to hourly variations in call numbers are linked to changes in sex ratios associated with egress and ingress from and to the spawning site, respectively. Specifically, RH2 was the most common call type during FSA. However, RH1 call type numbers peaked at the time of presumed spawning, while RH2 call type numbers decreased, confirming RH1 association with courtship display toward a female or a harem. At the interannual scale, the evolution of the relative variation of the two call types suggests either a significant change in the sex ratio tending toward a male dominated population or a spatial shift of the spawning site away from the location of the acoustic recorder. Understanding the relative role of call types and monitoring the relative variations of call type numbers in the reproductive dynamics of socially structured populations enables the understanding of potential changes in a spawning aggregation over time that could result from fishing pressure or environmental changes.

Introduction

Passive acoustics is a rapidly emerging field of fisheries management that has been gaining attention from fisheries scientists and managers over the last decade. While the most common application of passive acoustics has been to use sound as an aid in locating fish to study their habitat and behavior (Rountree et al. 2006), more recently a new field of passive acoustic is rapidly emerging in fisheries management (Luczkovich et al. 2008a, Gannon 2008, Aalbers and Sepulveda 2012, Parmentier et al. 2018, Di Iorio et al. 2020, Stratoudakis et al. 2024). Indeed, passive acoustics provides the capability of continuous long-term monitoring as well as remote monitoring. Such long-term monitoring can provide important information on daily, seasonal, and interannual activity patterns of fishes and other marine organisms. This is particularly true for fish that produce sound during reproductive activity. Those courtship-associated sounds (CASs) are, for most species, only produced during reproductive periods and therefore, can be used to monitor the reproductive activity of fishes. For some species that aggregate to spawn including Epinephelids and Sciaenids, the predictability of their spawning aggregation makes them vulnerable to overfishing (Sadovy de Mitcheson 2016, Heyman et al. 2019). As an example, long-term passive acoustic monitoring (PAM) of the meagre (*Argyrosomus regius*) spawning aggregation in Portugal and concurrent daily commercial fishery data such as catch per unit effort data were combined to establish management measures of the fishery where sound is used as catch indicator (Stratoudakis et al. 2024). In the study herein, we analyzed more than a decade of CAS recordings at a red hind (*Epinephelus guttatus*) spawning aggregation on the shelf break of a Caribbean Island. While most PAM studies monitoring indicators are based on sound pressure levels (SPLs) of sound production or choruses in the frequency range pertaining to the species of interest, we instead analyzed the long-term evolution of CAS call types and used them as indicators of changes in the spawning population.

The red hind is a midsized, long lived, slow growing grouper that inhabits shallow coral reefs 3–180 m deep from North Carolina, USA to the central coast of Venezuela. It is a com-

mercially important fishery in the West Indies including Puerto Rico (Matos-Caraballo and Sadovy 1990, Matos-Caraballo 1997), the US Virgin Islands (USVI) (Beets and Friedlander 1998), the British Virgin Islands (Eristhee et al. 2006), the Northeastern Antilles (Munro and Blok 2005, Nemeth et al. 2008, Kadison et al. 2009), Jamaica (Munro et al. 1973), and Bermuda (Luckhurst and Trott 2008). Red hind is a protogynous hermaphrodite in which individuals function first as females and then as males (Shapiro, 1987).

This species forms spawning aggregations annually at recurring locations and times (Shapiro et al. 1993, Sadovy et al. 1994b, Beets and Friedlander 1997, 1999, Whiteman et al. 2005, Nemeth 2005) with high site fidelity and predictability of the fish spawning aggregations (FSAs), which makes them especially vulnerable to exploitation (Domeier and Colin 1997). Red hind spawning aggregations consist of hundreds to tens of thousands of fish, which migrate up to 33 km or more from their home reef to reproduce (Nemeth 2005). At the onset of the aggregation, males arrive to an extended area to establish and defend territories from other males (Whiteman et al. 2005, Nemeth et al. 2007). They exhibit distinct body colorations and also display courtship behaviors toward females (Colin et al. 1987, Shapiro et al. 1993). This mating strategy is described as a lek-like behavior (Zayas-Santiago et al. 2020) and has been observed in other species such as the red grouper (*Epinephelus morio*; Nelson et al. 2011) and in Atlantic cod (*Gadus morhua*, Hutchings et al. 1999).

The spatial structure of red hind grouper aggregations consists of small harems with one male defending three to five females and spawning occurs in pairs or small groups of individuals 1–2 m above the seafloor (Shapiro et al. 1993). Four to five days before spawning females arrive and dominate sex ratios at the FSA site and in surrounding areas (Nemeth et al. 2007). Colin et al. (1987) suggest that males join clusters of females as they arrive to the sites, hence described as haremic. Two to three days before the full moon (DBFM) the sex ratio tends toward unity or becomes dominated by males (Colin et al. 1987, Nemeth et al. 2007) then becomes dominated by females the day of apparent spawning up to 2 days after the full moon (DAFM). Fish may disperse soon after spawning or some individuals remain on site until the following lunar cycle to spawn again (Sadovy et al. 1994b, Nemeth et al. 2007, 2008). At the red hind FSA of St. Croix, USVI, Nemeth et al. (2007) noticed that the largest males and females of the spawning population remained on site between subsequent spawning peaks.

Between one and three spawning events occur per season and are tied to the lunar and solar cycles (Nemeth et al. 2007). Spawning in the Caribbean is tied to the full moon and is associated with seawater temperature between 25°C and 27.5°C and concurs with periods of decreased current speeds at FSAs between December and February each year (Sadovy et al. 1994b, Nemeth et al. 2007, 2008). The timing of aggregation formation relative to the full moon varies between sites and within a site it varies following the winter solstice (Nemeth et al. 2007, Rowell et al. 2012, Appeldoorn et al. 2016). At the Red Hind Bank, St. Thomas (USVI), within a season, some lunar cycles have aggregations with higher densities than others, and this has been shown to vary across years with predictable temporal patterns relative to the number of days between the winter solstice and the January full moon (Nemeth et al. 2007) although in Puerto Rico there have been observations of divergence from this model (Appeldoorn-Sanders et al. 2023). When the January full moon occurs between 10 and 20 days after the winter solstice, January and February will be the primary months for aggregation. When the full moon occurs between 20 and 30 days, the aggregation forms primarily in January. If the full moon occurs between 30 and 40 days after the winter solstice, December and January will be the primary aggregation months.

Red hind are also soniferous and during their spawning aggregation, they produce sounds associated with reproductive behaviors, such as courtship, territorial, and harem defense (Mann et al. 2010). The production of sounds during reproduction has been observed for soniferous fishes in many families including Epinephelidae (Nelson et al. 2011, Schärer et al. 2012a, 2012b, 2014), Pomacentridae (Myrberg et al. 1986, Lobel and Mann 1995), Sciaenidae (Mok and Gilmore 1983, Ramcharitar et al. 2006), Gaddidae (Engen and Folstad 1999, Hawkins and Amorim 2000), and Batrachoididae (McKibben and Bass 1998, Fine et al. 2001). Some species exhibit different sounds with specific reproductive behaviors (Winn et al. 1964, Mok and Gilmore 1983, Connaughton and Taylor 1995, Mann and Lobel 1995, McKibben and Bass 1998, Johnston and Johnson 2000, Locascio and Mann 2008, Malavasi et al. 2009, Mann et al. 2010, Nelson et al. 2011) including red hind (Zayas-Santiago et al. 2020).

Red hind produce sounds associated with reproductive behaviors that are only observed when they aggregate to spawn and are mainly produced by males during courtship displays toward gravid females and territorial/harem defense with other males (Mann et al. 2010). Females are also capable of sound production as shown by Zayas-Santiago et al. (2020) in captivity. Males produce at least three distinct stereotypical sound types that are common during FSAs and were also detected in captivity during the week prior to spawning (Wilson et al. 2020, Zayas-Santiago et al. 2020, Appeldoorn-Sanders et al. 2023). The first call type, RH1 is a combination of one or two pulses followed by a pulse train with increasing interpulse period (Fig. 1a) with frequency range 20–360 Hz. The second call type, RH2 is generally composed of a pulse train followed by an extended tone in the same frequency range as RH1 (Fig. 1b). The tonal part duration can vary and the RH2 call is nonetheless substantially longer than RH1 with a duration of >3 s in average versus 2 s for RH1 (Wilson et al. 2020). The third type of call is named grunt/grunt train, RH3, and can be seen as a single grunt or grunt train mostly consisting of two or three successive grunts (Fig. 1c). It is this call that was shown to be produced by a female (Zayas-Santiago et al. 2020). The fourth type of call is the pulse/pulse train. This call can be produced as multiple consecutive pulses that can be found alone or as part of other type of calls, usually before or after another call such as RH1 or RH2. Fig. 1d shows consecutive short pulses (RH4), resulting in a pulse train without any other type of calls. The frequency range of RH3 and RH4 is greater than the previous two calls, between 20 and 500 Hz. Their durations also vary depending on the number of pulses or grunts that are produced but generally do not exceed 3 s.

The behavioral context associated with each of the four call types was described in depth by Zayas-Santiago et al. (2020). Observations in captivity revealed distinct scenarios associated with each call type. The most common call types, RH1 and RH2, were associated with reproductive displays of different interactions, where RH1 was heard when a male swam over to court a female, whereas RH2 was associated with harem defense or when a rival male was present. Male–

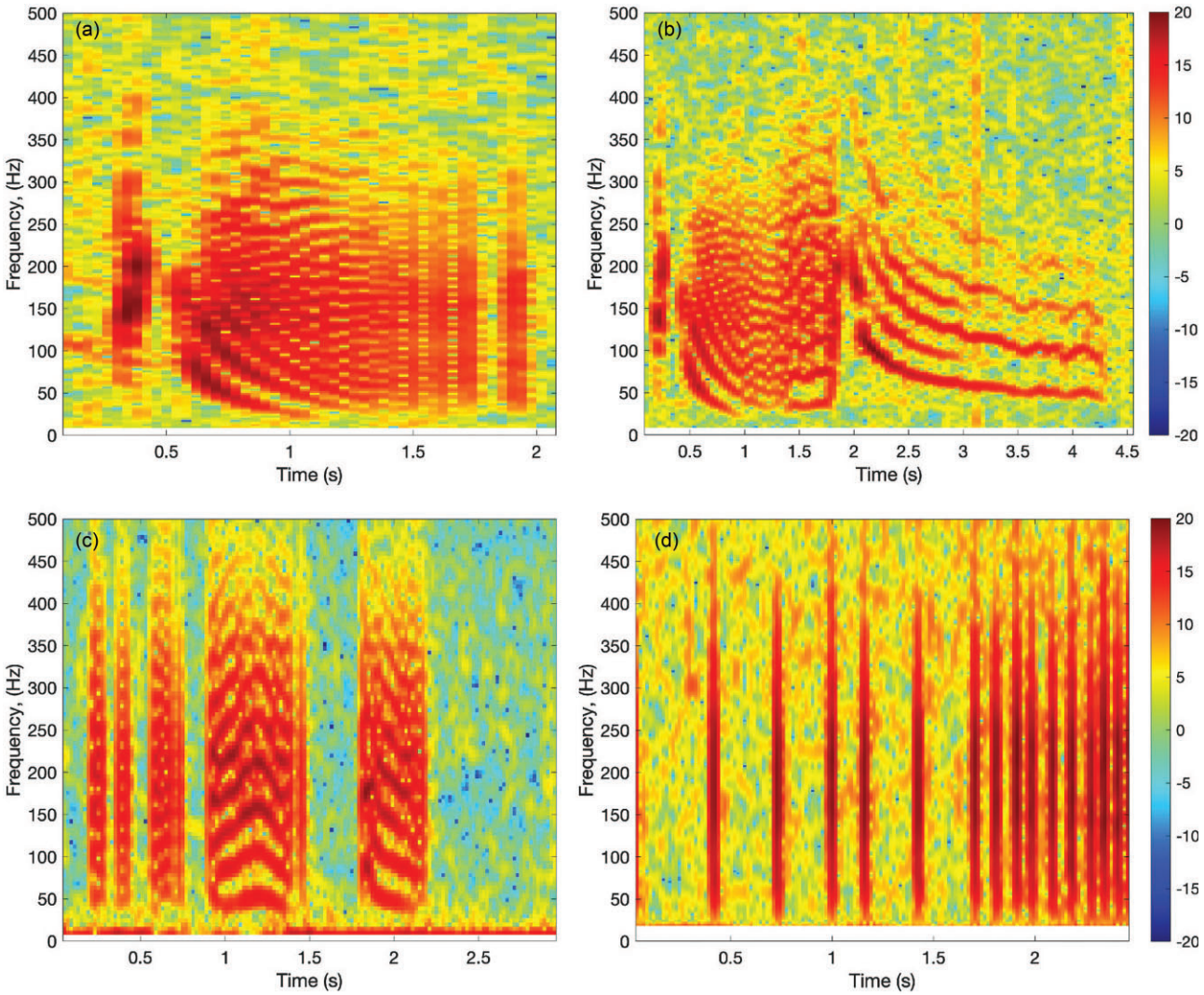

Figure 1. Red hind call types. (a) RH1, which consists of a pulse followed by a pulse train of increasing interpulse interval, (b) RH2, a pulse train followed by a tone, (c) RH3, a grunt train, and (d) RH4, a pulse train.

male interactions were observed when RH3 and RH4 were detected, while the latter was presumed to be produced by a female. Passive acoustics monitoring (PAM) of red hind sounds has thus been used to locate FSAs (Appeldoorn et al. 2014, Chérubin et al. 2020, Woodward et al. 2023) and to identify the temporal dynamics of these aggregations.

Long-term monitoring by Mann et al. (2010) and Rowell et al. (2012) in Puerto-Rico revealed the peaks in SPLs in the 100–200 Hz band between January and March. It was shown to be from red hind aggregating near the hydrophones at the FSA site, associated with the lunar cycle and exhibited a diel pattern. Sound production by red hind increased toward the day(s) of presumed spawning, which varied from 0 to 13 DAFM at Abrir la Sierra (ALS) off western Puerto Rico. In contrast, peaks in red hind density were shown to occur 0- to 4-DBFM at the red hind FSA south of St Thomas, USVI (Nemeth 2005, Nemeth et al. 2007). Peaks in CAS were followed by a decline in acoustic activity, suggesting a reduction in reproductive-related behaviors (Mann et al. 2010, Rowell et al. 2012, Appeldoorn et al. 2016).

Red hind also exhibit a chorusing acoustic behavior during their spawning aggregation that has been shown to only occur once per day at dusk and over a maximum period of 3 h (Appeldoorn-Sanders et al. 2023). As daily CAS rates increase approaching the presumed spawning nights, calls become continuous and overlapping in a *crescendo*, forming the "chorus" (Zayas-Santiago et al. 2020), which has been deemed as an indicator of imminent spawning (Appeldoorn-Sanders et al. 2023). These chorusing periods were identified by the maximum SPL values during those times, with intensity at least 10 dB higher and a dominant frequency 100 Hz lower than the ambient soundscape at dusk when chorusing was absent. Days when chorusing was present occurred mostly in clusters of three or more successive days, while the duration of chorusing peaked at some point during that period. Appeldoorn-Sanders et al. (2023) suggest that sunset times influence the red hind calling behavior on a seasonal scale, and it has been suggested as a possible cue for synchronized spawning (Nemeth 2009). The only observation of red hind spawning to date were 30 and 5 min prior to sunset in La Parguera, southwest Puerto Rico (Colin et al. 1987) where one female and one male rose 0.5 m from the seafloor to release gametes and were joined by a second female. The reproductive and acoustic behaviors of Gulf grouper *Mycteroperca jordani* show similarities

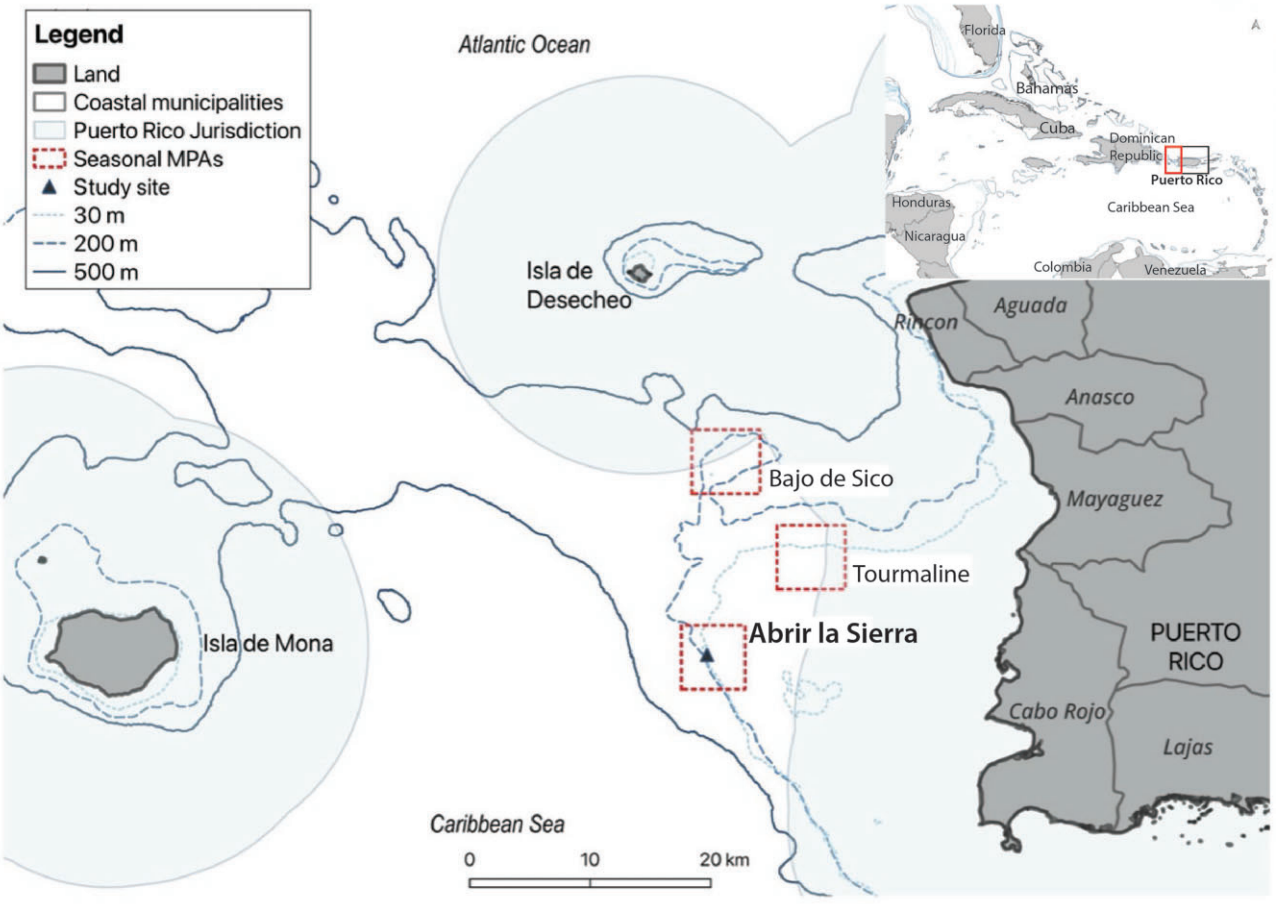

Figure 2. Map of western Puerto Rico and three seasonal MPAs with the study site at ALS.

with the red hind. Adult *M. jordani* also display a lek mating system in which large males formed territories over sand adjacent to a rocky reef where females moved into male territories during evening hours to spawn (Rowell et al., 2018). Sounds associated with spawning rushes, prior to gamete release were documented and sound production increased toward peak spawning hours. Sound production associated with spawning is not unique to Epinephelids. It is been observed in red drum *Sciaenops oceallatus* spawning aggregations where calls consisting of at least eight pulses per calls are associated with spawning (Lowerre-Barbieri et al. 2008). Rowe et al. (2006) described a sound as a "hum," which was produced when a male and female cod *Gadus morhua* swam together in a formation that led to spawning. Spawning at red hind aggregations sites where PAM is ongoing has yet to be observed, and the fish behaviors during chorusing are unknown.

Daily variations and diel patterns of relative call type production across multiple spawning periods are yet to be described and may further illuminate the significance of the call types throughout the dynamics of the FSA. This study analyzed 12 continuous years of sound recordings at the ALS FSA to describe the relative temporal variation of RH1 and RH2 call types. We suggest that the shift in the proportion between the two dominant call types (RH1 and RH2) over the spawning period may provide further information on their perceived purposes relating to agonistic interactions between males or response to harem formation by females, respectively. Interannual variations of the ratio between call types may also be indicative of overall changes in the red hind spawning population at ALS monitoring site, such as a change in the sex ratios or in the location of the nucleus of the spawning site.

Methods

Data collection and processing

The sound recordings used in this study were collected at ALS where red hind are known to aggregate to spawn (Fig. 2). This FSA is located within one of three seasonally closed marine protected areas (MPA) off western Puerto Rico (Schärer-Umpierre et al. 2014). These three MPAs were established in 1996 to protect red hind spawning stocks, and ALS is closed to all fishing from 1 December to 28 February each year.

The PAM conducted at the study site since 2007 consists of the deployment of at least one acoustic recorder at a location which has been identified as the midpoint of the area where densities of red hind are higher than background (Rowell et al. 2010). The midpoint of the FSA was previously identified through repeated drift surveys during late afternoon and early evening hours where a hydrophone was lowered from a surface vessel in the water column. The repeated surveys over the ALS FSA were used to map the calls distribution of red hind during presumed spawning hours and the location of the highest density of calls was selected as the location of the acoustic recorder. The recorder's location was about 500 m from the shelf edge at 24 m depth, which is at the midpoint of an area ~500 m long where red hind density is up to 40 times

higher than background during the aggregations, and it is the only species known to aggregate at this location (Rowell et al. 2012).

The recordings used in this study encompass the period 2011–2022 and were obtained with Loggerhead Instruments Digital Spectrogram recorders (DSG), that were deployed for 6 months from December to May each year to encompass the red hind spawning season and its temporal variability. The sampling rate varied between 44.1 and 80 kHz, and a duty cycle of 20 s every 5 min was set for each recorder, which yielded more than half a million acoustic files. Because of the high volume of acoustic data generated in our study, we used the fish acoustic detection algorithm research (FADAR) software (Ibrahim et al. 2018a, 2019, 2024) to conduct automatic red hind classification of CAS types.

FADAR (Ibrahim et al., 2024) is a Matlab executable program that uses an ensemble of convolutional neural networks (CNN) to detect and classify the CAS of four grouper species, including differentiating between within-species CAS types with species specific deep learning algorithm. Unlike conventional machine learning classification algorithms, FADAR does not rely on sophisticated preprocessing and hand-crafted feature extraction procedures. In fact, deep learning models act as both feature extractors and classifiers (Zhang et al., 2017). CNNs are especially effective in identifying spatial patterns from images. Therefore, spectrogram images of the audio files from the DSGs (Fig. 1) are used as input to FADAR, rather than the sound signal itself after denoising of the signal by a discrete wavelet transform (Ibrahim et al. 2018a). FADAR accuracy has been assessed in previous work (Ibrahim et al. 2018a, 2019, 2024) as part of the evaluation of the species-specific algorithms that are used in FADAR. This algorithm can identify seven CAS types of different Atlantic Ocean grouper species in their natural environment with a classification accuracy above 90%. Van Horn et al. (2024) applied FADAR to the analysis of Nassau grouper movements during spawning aggregation using an array of six hydrophones. Half were Loggerhead DSGs and half were Ocean Instruments SoundTrap recorders, with different sensitivities, sampling rates and gain settings. FADAR accuracy was evaluated on this set of recorders by comparing the results of FADAR and a manual classification on randomly chosen audio samples. Their results showed that FADAR reached an accuracy of 85.6% with new data collected in the Cayman Islands for Nassau grouper call types.

In this study, a similar approach was followed in which FADAR's accuracy was measured as the rate of misclassification, i.e. the number of false positives (FP) and false negatives (FN), by conducting manual detections of red hind grouper call types in spectrograms created in Audacity (version 3.4.2) on 100 randomly chosen files for each spawning season that have at least one red hind grouper call of any type. The misclassification rate, calculated as $(FP + FN)/T$, where T is the total number of detections (true positive), was used as a measure of FADAR's detection error for each season. The error is shown as a shaded area in the CAS types time series.

Call counts and assumptions

In order to create hourly time series of standardized call rates across spawning season and years, the number of detects of each call type (RH1 and RH2) were summed for the total 4 min of recordings within each hour. That number was then multiplied by 15 under the assumption that a measured call rate within any given hour would be consistent throughout that hour (Rowell et al. 2012, Chérubin et al. 2020, Woodward et al. 2023). Daily CASs are the sum of the hourly detects over a 24-h period, which provided the time series of daily CAS types for each year.

An important assumption is regarding the presumed listening area. Chérubin et al. (2020) estimated that the detection range of red hind CAS was at best 100 m given the background noise at Red Hind Bank in the USVI. Therefore, we also assume that the red hind CAS detection range is 100 m from the hydrophone in all directions. This distance constitutes a subportion of the greater FSA area at ALS. And although the acoustic recorder is deployed in the same position year after year, the fish move when they arrive each year, therefore they could disperse and set up territories differently around the recorder.

Data analysis

Interpolated CAS were grouped by factors according to DAFM, season year (i.e. spawning season year 2014 spanned from December 2013 to May 2014), and lunar cycle (i.e. whether the measurement fell within the first or second spawning event of its respective season). Euclidean distances were then calculated for both RH1 and RH2 detections, and a permutational analysis of variance (PERMANOVA) was conducted in Matlab (R2023a) via the Fathom Toolbox (Jones 2017) with DAFM, season year, and lunar cycle as fixed factors of 16, 12, and 2 levels respectively. The PERMANOVA was conducted with 999 permutations.

Finally, for each spawning season, RH1 and RH2 CAS estimates were averaged in 4-hourly blocks (0:00–3:00, 4:00–7:00, 8:00–11:00, 12:00–15:00, 16:00–19:00, and 20:00–23:00) for each day of the 0–15 DAFM window to assess the presence or absence of the dusk (16:00–19:00) calling peak presumed to precede spawning. Colin et al. (1987) observed spawning only twice, within 30 min before to sunset. Hourly time series of RH1 and RH2 were further compared with the presence of chorusing that was also quantified in this study under the hypothesis that choruses may mask the detection of RH1 calls during dusk hours on the days of peak calling activity.

As shown in Appeldoorn-Sanders et al. (2023), chorusing usually occurs on days of peak calling activity associated with courtship behaviors that precede spawning. Chorusing is characterized by continuous overlapping calls dominated by RH1 (Zayas-Santiago et al. 2020). Since the individual calls become almost undistinguishable during chorusing events in a spectrogram it could decrease the detector's capacity to identify the calls. Chorusing times were thus obtained from Appeldoorn-Sanders et al. (2023) who analyzed the same data used in this study.

Visual drift census surveys

Starting in 2007, drift dive surveys of the same study sites were conducted to quantify red hind densities, both near ALS as well as in neighboring habitat along the shelf break. Following the survey methods of Rowell et al. (2012), divers counted each grouper observed within 2 m about a centerline transect in a pre-established 400 m long by 100 m wide area, recording approximate length and observation time for each individual. Their potential spawning condition and behaviors (e.g. dis-

Table 1. PERMANOVA of the significance of DAFM, the lunar cycle and the season year on the RH1 and RH2 calls

RH1					
	df	**SS**	**MS**	**Pseudo-*F***	***P*-value**
DAFM (1)	15	8.4e + 07	5.6e + 06	144.4	.001
Lunar Cycle (2)	1	2.1e + 07	2.1e + 07	542.4	.001
Season Year (3)	4	1.8e + 07	4.4e + 06	113.5	.001
1 × 2	15	7.9e + 06	5.3e + 05	13.5	.001
1 × 3	60	5.1e + 07	8.5e + 05	21.7	.001
2 × 3	4	3.6e + 07	8.9e + 06	228.6	.001
1 × 2 × 3	60	1.8e + 07	3.0e + 05	7.8	.001
Residual	3680	1.4e + 08	3.9e + 04		
Total	3839	3.8e + 08			
RH2					
DAFM (1)	15	5.7e + 07	3.8e + 06	155.8	.001
Lunar Cycle (2)	1	1.3e + 07	1.3e + 07	551.7	.001
Season Year (3)	4	8.3e + 07	2.1e + 06	841.3	.001
1 × 2	15	1.9e + 06	1.3e + 05	5.2	.001
1 × 3	60	2.5e + 07	4.2e + 05	17.1	.001
2 × 3	4	2.1e + 07	5.4e + 06	218.5	.001
1 × 2 × 3	60	7.1e + 06	1.2e + 05	4.8	.001
Residual	3680	9.0e + 07	2.4e + 04		
Total	3839	2.9e + 08			

sdf, Degrees of Freedom; SS, Sum of Squares; MS, Mean Sum of Squares. Significance values are based on 1000 permutations

tention and coloration) were also noted. Time of observation was used to determine location using GPS measurements from a handheld situated on the diver's surface buoy. Red hind density (number of fish 100 m^{-2}) was calculated for each survey by dividing the total the number of red hind by the total area surveyed. Mean fish density and standard deviation was calculated from the two transects when available and will be compared to the evolution of CAS on the same day as the surveys.

Results

Interannual monthly variability of overall CAS rates

Over 2000 h across 12 years of acoustic recordings at ALS were analyzed for red hind CAS types. The PERMANOVA output (Table 1) shows high significance for all factors and each combination of interactions. These results indicate that differences in CAS across years are contingent on both the lunar cycle within that season as well as the DAFM within each cycle. Call type rates appear to follow the lunar cycle, which dictates the monthly variations across each spawning season (Fig. 3). The temporal variation of both RH1 and RH2 reveals a consistent increase from mid-December, reaches a maximum in January for most years, and is followed by a secondary peak in February, of smaller magnitude than in January, except in 2016 and 2021 when the latter peak was slightly greater than in January. In 2018, 2020, and 2022, the February CAS peak was of similar magnitude as the January one. The timing of the peaks follows, for the most part, the peak aggregation month(s) prediction model of Nemeth et al. (2007) with some exceptions (Table 2).

The timing of peak CAS shown in Table 2 confirms the predictability of the timing of the spawning period at ALS as done by Nemeth et al. (2007) at Red Hind Bank, USVI, although with a few exceptions. In 2013 and 2019, when two major peaks were expected, only one was higher in CAS detections. In 2019, the CAS numbers peaked twice in January, around 15 and 23 DAFM. In 2020, while the model predicted one peak month, two were observed, one in January and one in February. In all other years, except 2022, CAS numbers peaked between 0 and 15 DAFM.

Appeldoorn-Sanders et al. (2023) analyzed the red hind choruses over the same years and noticed the same shift in chorusing months. When choruses occurred, their time matched peak CAS times, which suggests that choruses are associated with peak CAS detected by FADAR. In 2021, CAS peaked three times and correspond to the three chorusing periods shown in Appeldoorn-Sanders et al. (2023). However, peak CAS occurred when choruses were not present as well, for example in February 2017 and 2019. These peaks were lower than the January CAS peak, when choruses occurred.

Over the 12-year period presented in Fig. 3 a gradual increase in the magnitude of RH1 CAS and a sudden rise in RH2 CAS are evident in the 2011–2017 period (Fig. 4). In 2011 and 2012, the RH2 CAS type was always greater than RH1 and peak RH2 CAS were lower than 15 000 calls. Starting in 2013, RH1 CAS type became greater than RH2 during the peak CAS periods. CAS jumped to nearly 24 000 in 2013. It remained close to the same level in 2014 and peaked to almost 27 000 in 2015. That number dropped back to just below 20 000 in 2016 and reached 22 000 in 2017. Starting in 2018, the RH2 CAS type became significantly greater than RH1 over the spawning season. In 2018, peak RH2 CAS type reached 22 000 and in 2019, the RH2 CAS type reached close to 27 000, dropped to 25 000 in 2020 and 2021 before reaching again 27 000 in 2022. In summary, the number of RH2 CAS calls nearly tripled over a 12-year period. RH1 CAS numbers instead reached 9000 in 2018 and increased to a peak of about 13 000 the following years.

Relative variation of CAS type rates at the hourly and seasonal scale

The pattern of increasing CAS types during each lunar period seems to follow the gradual increase in red hind abun-

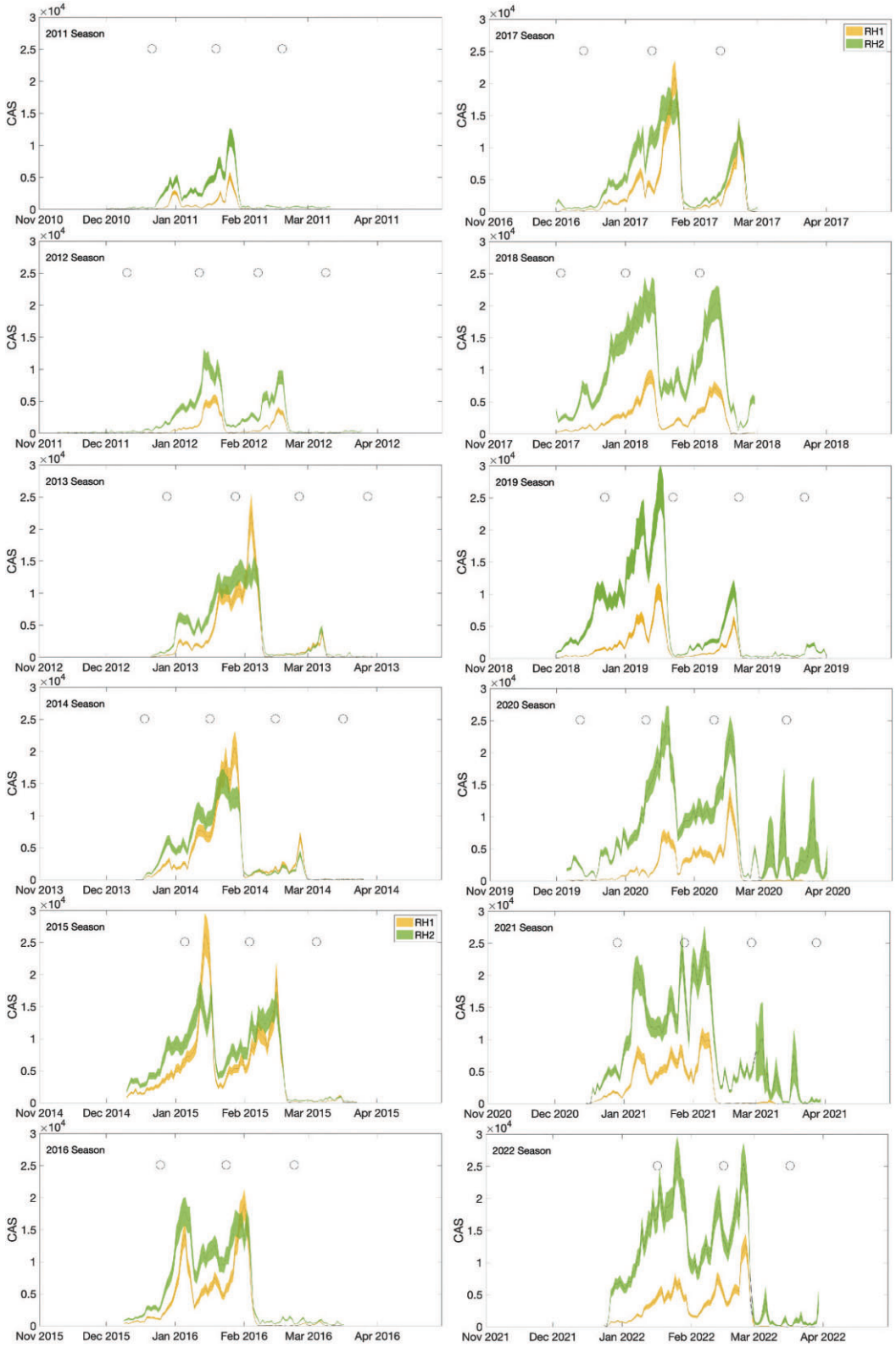

Figure 3. Daily interpolated RH1 (solid line, yellow) and RH2 (dotted line, green) CAS (counts d^{-1}) over each reproductive season of *E. guttatus* between 2011 and 2022 at Abrir la Siera FSA. The shaded areas show FADAR's misclassification error. Black circles show the full moon.

dance over the same lunar time periods at FSA sites in general (Colin et al. 1987, Shapiro et al. 1993, Whiteman et al., 2005, Nemeth et al. 2007, 2008, Rowell et al. 2012, Zayas-Santiago et al. 2020, Appeldoorn-Sanders et al. 2023). Namely, as the number of fish, first males, then females, increases at the aggregation site, the number of CAS per day increases as well and then abruptly drops to almost 0 at the end of each spawning aggregation peak. This would align with the observation of

Table 2. Comparison of peak predicted spawning months by Nemeth et al.'s (2007) model and observed calling peaks. Row color indicates a repeat in the number of days after the winter solstice. Each color corresponds to a different winter solstice elapsed period. Rows with two tones of the same color indicate that only one peak calling month instead of predicted two

Year	Number of days after the winter solstice	Nemeth et al. 2007 primary aggregation month(s) prediction (4-0 DBFM)	Peak CAS numbers month(s)	Full moon day December	Full moon day January	Full moon day February
10-2011	20-30	January	6-10 DAFM January	21	19	18
11-2012	10-20	January - February	3-11 DAFM January – 6-13 DAFM February	10	9	7
12-2013	30-40	December - January	7-13 DAFM February	28	27	25
13-2014	20-30	January	8-15 DAFM January	17	16	15
14-2015	10-20	January - February	9-16 DAFM January 10-16 DAFM February	6	5	4
15-2016	30-40	December - January	9-16 DAFM January 6-15 DAFM February	25	24	22
16-2017	20-30	January	6-14 DAFM January	14	12	11
17-2018	10-20	January - February	9-15 DAFM January 8-14 DAFM February	3	2	Jan. 31
18-2019	30-40	December - January	14-27 DAFM January	22	21	19
19-2020	20-30	January	6-14 DAFM January 6-12 DAFM February	12	10	9
20-2021	30-40	December - January	7-15 DAFM January 8-14 DAFM February	30	28	27
21-2022	30-40	December - January	8-13 DAFM January 8-13 DAFM February	19	18	16

most fish leaving the aggregation, in particular when there is only one primary spawning month as observed by Rowell et al. (2012) and as seen in 2013, 2014, and 2019. The CAS type variation, while it follows the seasonal trends, shows some relative changes during each spawning month. Zayas-Santiago et al. (2020) showed in their analysis of the call type variation during the month of January 2017 that during the period 0–12 DAFM, the number of RH1 CAS type increased toward the middle of that period and became greater than the RH2 for a few days. Our results reveal that the RH2 CAS type is the most common one at the onset of each aggregation period as shown by Fig. 3. However, between 2013 and 2017, while RH2 CAS number increased toward peak spawning activity, the number of RH1 CAS overtook the number of RH2 CAS type detections (Fig. 3), during the 5–15 DAFM period (Fig. 5).

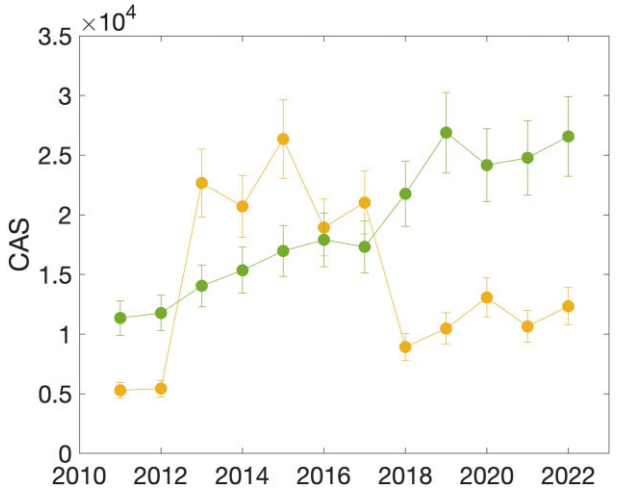

Figure 4. Annual peak CAS (counts d^{-1}) for RH1 (yellow) and RH2 (green) CAS over each reproductive season of *E. guttatus* between 2011 and 2022 at Abrir la Siera FSA. The error bars show FADAR's misclassification error.

We found considerable diurnal variation in RH1 and RH2 CAS for each spawning month (Fig. 5). In 2013, when peak CAS were in February (Fig. 5a), the hours of peak RH1 sound production were in the 20:00–23:00 AST window between 1 and 5 DAFM, then switch to the 16:00–19:00 AST period primarily between 6 and 13 DAFM. Secondary peaks were observed in the 20:00–23:00 and 0:00–7:00 periods in particular between 7 and 10 DAFM. During the second peak of CAS numbers in March 2013, the main calling hours for RH1, also above the call numbers of RH2, were around sunset in the 16:00–19:00 (Fig. 5a).

A similar pattern is observed in 2014, although the month of peak CAS is January (Fig. S1). RH1 exhibit the highest CAS numbers, starting on 5 DAFM in the 20:00–23:00 window, then shifted to the 16:00–19:00 window from 8 to 15 DAFM. The second highest RH1 call numbers were in the 0:00–7:00 h window. In February 2014, a peak in RH1 CAS numbers also occurred in the 16:00–19:00 window from 9 to 14 DAFM. In 2015, the peak in RH1 CAS numbers overpassed RH2 numbers on 8 DAFM until 13 DAFM in the 16:00–19:00 window. During the second spawning month of 2015, the highest number of RH1 call were seen during the 16:00–19:00 period from 10 to 16 DAFM. Nighttime RH1 CAS numbers were not higher than RH2 CAS numbers. In 2013 and 2014, during the second peak of RH1 CAS numbers, RH2 CAS numbers remained relatively very low, and no chorusing were observed (Appeldoorn-Sanders et al. 2023). In 2015, RH2 numbers were relatively high, and chorusing was present during the second aggregation month (Fig. S2).

In 2016, the highest numbers of RH1 call type during the January aggregation were only observed during the 16:00–19:00 window from 9 to 16 DAFM, which is when choruses were also recorded. Greater numbers were observed during the February aggregation during the same period. RH1 daytime calling became more significant in 2015 and 2016, in both spawning months, especially on the day of peak RH1 calling in the 16:00–19:00 period (Figs. S2 and S3). In 2017, the highest RH1 call numbers were observed from 16:00 to 19:00 as in previous years (Fig. S4) both in January and February. RH1 calls, were also prominent in the nighttime, higher in numbers than RH2 calls. Peak calling occurred between 6 and 13 DAFM in January and February. A common pattern to all those years is the decrease in RH2 call numbers during peak RH1 calling hours, from 16:00 to 19:00.

Starting in 2018, the pattern of RH1 and RH2 CAS type numbers changed notably from the previous 5 years, despite the presence of choruses in the 16:00–19:00 period as shown in Appeldoorn-Sanders et al. (2023). From 2018 to 2022, the RH1 CAS numbers were no longer greater than RH2 at the peak of the RH2 CAS production (Fig. 4). In 2018, the relative CAS distribution by hours had changed and peak RH1 call numbers no longer occurred in the 16:00–19:00 period but instead in the 20:00–23:00 window (Fig. 5b). The RH2 CAS numbers no longer exhibited a decrease during the 16:00–19:00 period. This trend continues into the following years where the time of peak RH1 CAS numbers is seen during daytime hours as in February 2019 (Fig. S5), early morning hours in January 2020 (Fig. S6) and February 2021 (Fig. S7), late morning in January 2021 and 2022 (Figs. S7 and S8), or late evening hours in February 2020 (Fig. S6) and even late night of February 2022 (Fig. S8). One exception though is in January 2019 when peak RH1 CAS numbers are in the 16:00–19:00 period on days 23 and 24 after the full moon (Fig. S5).

Despite the shifts observed in the hourly peak CAS numbers for RH1 starting in 2018, chorusing seems to have occurred at the same peak hours, between 17:00 and 21:00 as shown in Appeldoorn-Sanders et al. (2023). This would suggest that chorusing could have a masking effect on the detection of RH1 call types by FADAR, which is discussed in the next section.

RH1 call detection masking by chorusing

We estimated the time and duration of chorusing hours and overlaid the results on the hourly call rates of RH1 and RH2 to assess the potential effect of chorusing on RH1 and RH2 CAS type detection (Fig. 6). In 2017, at the peak chorusing hours, RH1 calls become significantly higher than RH2 CAS, and the peak in RH1 calls is associated with a marked decrease in RH2 CAS (Fig. 6a). This result suggests, that while chorusing is present, the detector can capture the increase in RH1 CAS, which aligns with the observations of the relative variation of the same call types in captivity reported by Zayas-Santiago et al. (2020). In subsequent years, this relationship is no longer present, where chorusing at the FSA site is associated with a decrease in RH1 CAS type detected by FADAR, while not correlated with the RH2 CAS variations. This may indicate that less RH1 CAS types are detected near the hydrophone, but chorusing remains detectable. The 2019 chorusing periods associated with the two major peaks in call numbers in January (Fig. 6b), show that chorusing is not necessarily related to increase in RH1 calls at ALS, which is opposite to what was observed in 2017. However, the two overlap during the two days when the peak in RH1 calls is during dusk hours (23–25 DAFM in January 2019).

Fig. 6 also reveals that the inverse relative variation of the RH1 and RH2 observed during chorusing hours in 2017 and before is also present during the time of higher RH1 call production in the 2018–2022 period. Fig. 6b, d, e, and f shows that RH1 continue to be associated for the most part with a drop in RH2 calls. Although no chorusing was observed during those events. This would suggest that some courtship interaction would be occurring during that time as well.

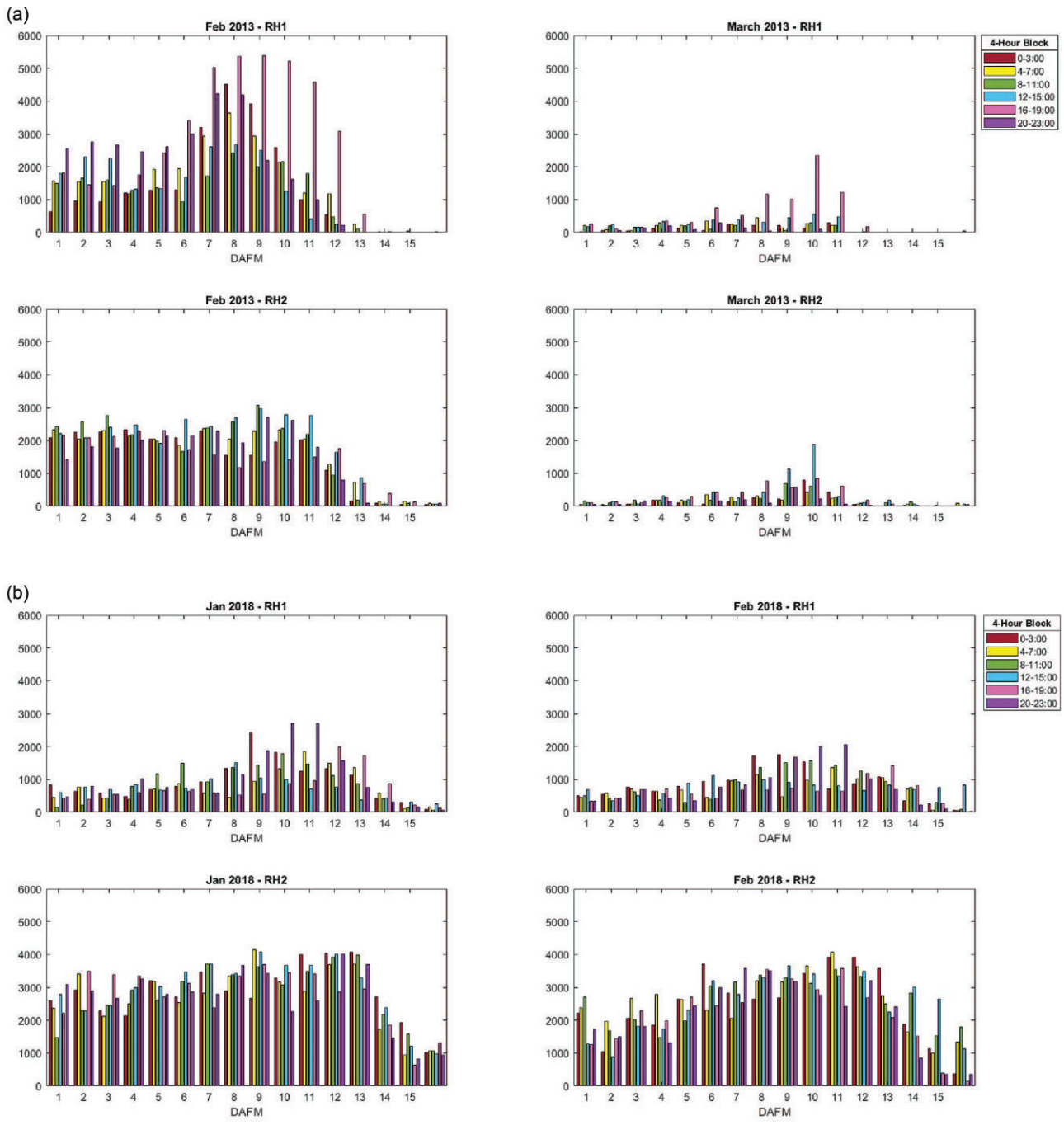

Figure 5. Four-hour block time series of RH1 and RH2 call type numbers for each spawning period [0–16 DAFM] of each month (January, February, and March if the main spawning peak is in February) for years 2013 (a) and 2018 (b), respectively. The pink color corresponds to dusk, hence the 16:00–19:00 h period. Each year is associated with four blocks corresponding to RH1 call type in the top row and RH2 call type in the second row. The time series corresponding to the other years are shown in the online Supplementary Material and are labeled Figs. S1–8.

CASs and fish density

The density estimates per day of underwater visual drift census surveys confirms that increases in CAS numbers are associated with increases in fish density (Fig. 7). As density increases, the difference between RH2 and RH1 CAS numbers also decreases, suggesting a density dependent effect. However, peak density is not necessarily associated with the RH2 and RH1 CAS peaks. In February 2013, fish density increased after the peak in CAS. In February 2017, fish density decreased, while CAS numbers increased. Despite these differences, the trend in fish density is parallel to the trend in CAS and the relatively faster increase of RH1 call types over RH2 CAS toward peak density and peak CAS numbers.

Discussion

This study provides a long-term (12 years), continuous sample of the red hind acoustic dynamics at ALS since all recordings were made at the same exact location, which is where the highest relative density of red hind was first observed in the ag-

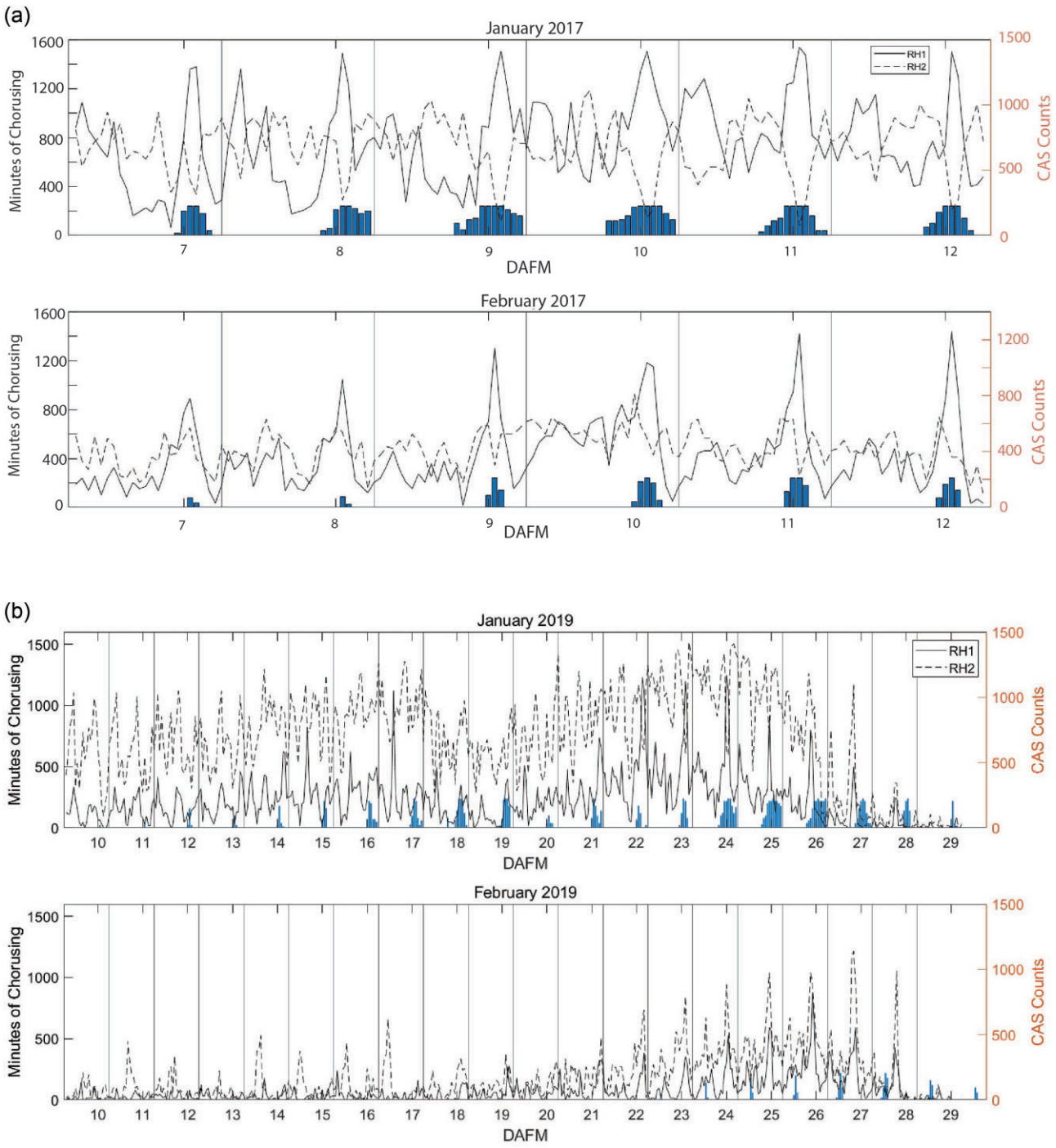

Figure 6. Hourly time-series of RH1 and RH2 call type numbers during the spawning weeks of years 2017 (a) and 2019 (b) spawning seasons. On the right-hand axis is shown the CAS counts and on the left-hand axis the minutes of chorusing shown for each hour by the blue bar plots. The tick mark associated with each day indicates the 18:00 h. The vertical line indicates the date change.

gregation area, and recorded with PAM since 2007 (Mann et al. 2010). Using FADAR, we analyzed large, multiyear acoustic data sets and identified important temporal patterns in red hind CAS at the ALS spawning aggregation site. These patterns included validating a temporal model of red hind timing of FSA formation among years (i.e. Table 2), identifying the relationship and variation in RH1 and RH2 call types among spawning seasons, months and diurnal time periods (i.e. Figs. 3–5), a progressive increase in red hind CAS numbers over the 12 year study period (i.e. Fig. 4), patterns among chorusing and RH1 and RH2 call peaks (i.e. Fig. 6) and a correspondence between monthly red hind CAS and red hind max density estimates (i.e. Fig. 7).

At the interannual scale, the analysis of the 12 spawning seasons spanning 12 years revealed that the prediction model of the main spawning month by Nemeth et al. (2007) was applicable to ALS. The model was originally devised for the Red Hind Bank FSA in St. Thomas, USVI, where red hind peak density during spawning months was observed 4–0 DBFM. When the full moon occurred late in the month, peak CAS

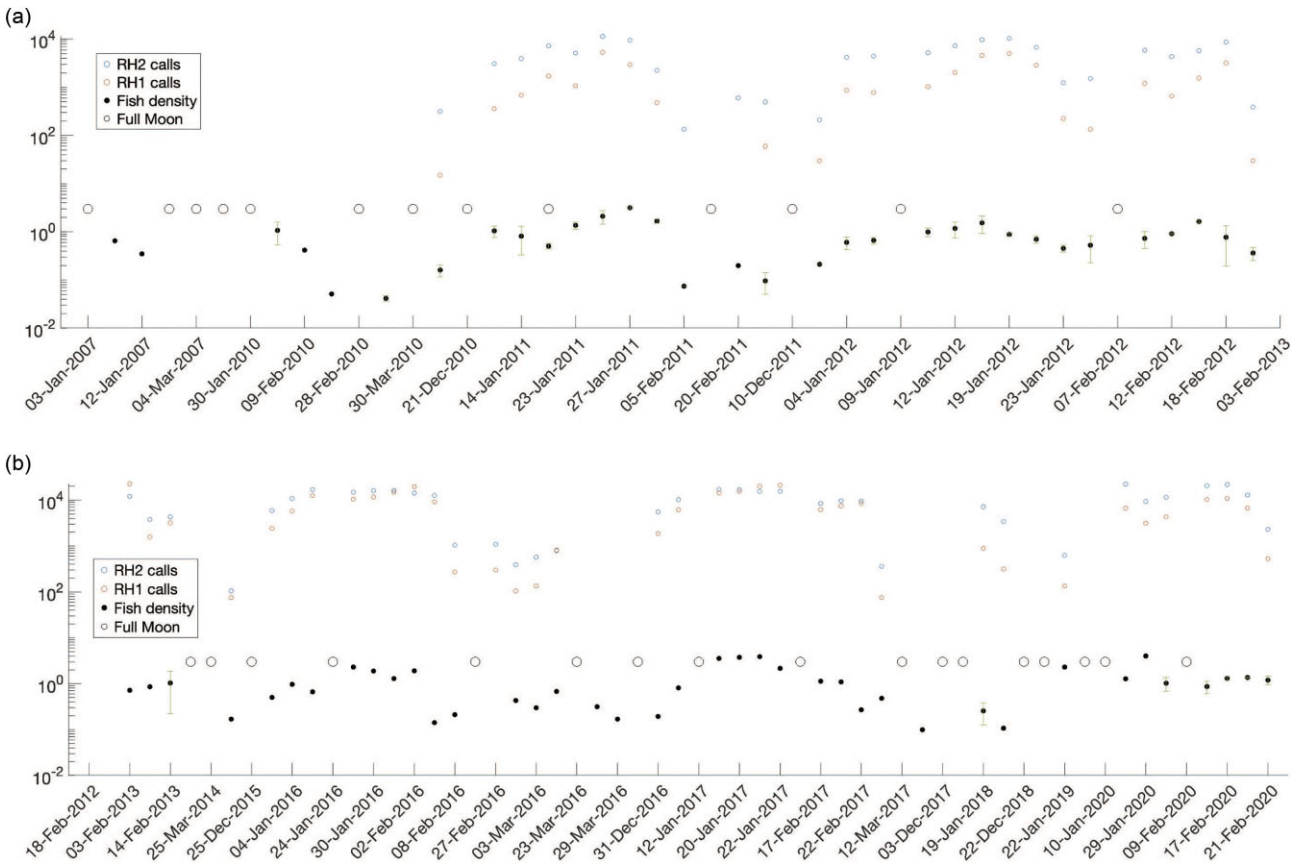

Figure 7. CAS counts overlaid on density estimates per day of underwater visual drift census surveys. The error bar is shown for surveys with more than one count. Please note that the max density day of each month/year may have been missed in years with fewer replicates. Black dots show the fish density as the average number of individuals per 100 m^2. Black circles show the full moon, blue circles the number of RH2 calls, and red circles the number of RH1 calls on the same day as the density estimates. The logarithmic scale is used on the y-axis.

would be expected the next month due to this offset. Peak CAS months in 2013, 2016, 2019, and 2021 would thus be in January and February instead of December and January, which matches the model's prediction. By adjusting for the fact that red hind density and CAS peak between 6 and 15 DAFM this model can still predict the peak aggregation months at ALS. Subsequently, one can hypothesize that peak CAS is associated with peak fish density at the FSA as suggested by Rowell et al. (2012).

The difference in timing related to the DBFM and DAFM that are observed between ALS and the Red Hind Bank (i.e. 5–0 DBFM, Nemeth 2005) have also been reported for Saba Bank, Netherland Antilles, St. Croix, USVI and Bajo de Sico, Puerto Rico. At Saba Bank red hind aggregated from 4 DBFM to 1 DAFM (Kadison et al. 2009). In St. Croix at the Lang Bank red hind FSA site, red hind densities peaked 3 DBFM to 3 DAFM (Nemeth et al. 2007) and at Bajo de Sico red hind gonad-somatic index peaked the week before the new moon or about 5–9 DAFM (Sadovy et al. 1994). These differences in timing may be due to the differences in density or population abundance. Whereas the maximum density estimated in drift transects for ALS is <4 indiv./100 m^2 (Fig. 7) compared to a mean maximum density of 40 at the Red Hind Bank (Nemeth 2005) and 35 at Saba Bank (Kadison et al. 2009). Population sizes were also considerably lower at Lang Bank, St. Croix than at Red Hind Bank, St. Thomas (Nemeth et al. 2006). A similar delay in the aggregation has been observed in the congener *E. striatus* where FSA with significantly higher abundances spawn on or near the full moon, whereas FSAs with lower total abundances show peak abundances later with relation to the full moon increasing their vulnerability to fishing as they spend more time overall on site (Heppell et al. 2014).

Deviance from the model was associated with a decrease in the number of spawning months on two occasions and an increase on one occasion. Appeldoorn-Sanders et al. (2023) found the same exceptions to the 30–40-day period based on the chorusing analysis. Although peaks in CAS were tied to chorusing activity in the 2013–2017 period, this relationship no longer holds in the 2018–2022 period as discussed further in this section. The temporal dynamics of the red hind FSA where fish progressively arrive and then leave all at once, after spawning, appears to align with the increase in sound production and CAS numbers as shown by Rowell et al. (2012) at ALS and Mona Island (Mann et al. 2010, Appeldoorn et al. 2013). We further showed that the increase in CAS is positively correlated with the fish density, especially during the buildup phase of the spawning aggregation.

At the seasonal scale, the CAS times series revealed two specific patterns in the relative numbers of RH1 and RH2 CAS. One in which RH1 CAS peaks were greater than RH2 during the spawning period and one where this difference was reversed. The former case is validated by the call type analysis of Appeldoorn et al. (2019). They analyzed the call type production during the lunar cycle of 11 January–13 February 2013

for a 1-h period, 18:00–19:00. During the days of higher than background sound production for a typical lunar cycle, they noticed B-type calls (RH2 herein) were most abundant from 0 to 6 DAFM, presumably the onset of the aggregation. This call decreased in abundance sharply and A-type calls (RH1 herein) increased from 7 to 12 DAFM, during the presumed spawning peak. During this latter time period, chorusing, indicative of high CAS activity, also increased. This pattern and timing in the relative variation of RH1 and RH2 is identical to the pattern seen in Fig. 5a. Zayas-Santiago et al. (2020) analyzed the CAS recording at ALS in January 2017 and showed that RH2 CAS numbers were greater 0–4 DAFM while RH1 CAS numbers were greater through 12 DAFM, which agrees with our results. Our analysis also shows that RH2 is the most common CAS type during spawning season, except for the spawning peak period, but only between 2013 and 2017. The density of red hind and CAS levels are known to increase during the build-up of the ALS aggregation (Rowell et al. 2012), and in the USVI, where most females arrive over the course of a few days (Whiteman et al. 2005, Nemeth et al. 2008). Based on Zayas-Santiago et al. (2020) captivity experiments, RH2 CAS numbers would increase because of the increased courting activity between male and harem, and male territorial defense against other males. Therefore, RH1 CAS type numbers would increase at a later stage during the spawning period toward peak spawning activity, overtake RH2 call numbers and decline rapidly afterwards as shown by Zayas-Santiago et al. (2020).

In February 2017, the ALS site was surveyed with a Wave Glider, an autonomous surface vehicle equipped with a PAM system that recorded red hind grouper CAS over the aggregation area in addition to the recorder deployed on the seafloor. Woodward et al. (2023) noticed that the CAS type captured by the Wave Glider during the spawning week of 2017 was mostly RH2, which suggest that RH1 and RH2 have different propagation characteristics. Hence it is possible that RH2 CAS could be used for longer range communications than RH1, whose sound production peaks during the spawning period, toward peak spawning activity as shown herein. RH2 was indeed shown to have the highest SPL in captivity (Zayas-Santiago et al. 2020). This call type may ultimately serve to keep males from entering other males' territories, as part of the behaviors observed include "arching" where males pose higher (1–2 m) above the seafloor to warn neighboring males in territorial displays (Nemeth 2012). As suggested by Appeldoorn-Sanders et al. (2023), not only chorusing but also RH1 may stimulate hydration prior to gamete release or synchronize spawning (Tavolga 1971, Lobel 1992, Biggs and Erisman 2021). This may occur across multiple harems over the extended area of the FSA sites that are distributed along the western shelf of Puerto-Rico as shown by Woodward et al. (2023). This would also explain as well, the synchronized spawning across the Red Hind Bank, in the USVI, which consists of multiple small FSAs as shown by Chérubin et al. (2020).

At hourly scales, the diel cycles of CAS consist of a peak near dusk with a smaller peak near dawn, all call types considered, with the lowest number of calls being observed around midday and midnight as shown in previous studies (Mann et al. 2010, Rowell et al. 2012, Zayas-Santiago et al. 2020). The diel patterns revealed that RH2 CAS were more frequent on average over a 24-h period between 0 and 13 DAFM, except during dusk in the years 2013–2017. Peaks in RH1 CAS, and above RH2 CAS were specifically occurring at dusk in the 16:00–19:00 period, this includes sunset, when red hind have been observed to spawn in Puerto Rico (Colin et al. 1987).

The significant changes observed after 2017 in the relative numbers of CAS types could be explained by several factors, and we propose to explore two of them. The first factor is associated to a relative increase in male abundances that resulted in a long-term shift in sex ratios, without a decrease in spawning biomass, or a possible increase, which the increase in CAS over the years suggests. The significant decrease in RH1 (from 26 to <15 000) may indicate a decrease in the number of direct courtship events and male/female interactions. Subsequently an increase in RH2 could signify higher competition (male/male interaction or chasing) or the need to attract females that are not in proximity or in relative high abundance. Starting in 2019, in 2021 and 2022 more than two CAS peaks were observed with associated chorusing (Fig. 6), suggesting that spawning days relative to the full moon may have changed as well, although RH1 CAS numbers never peaked over RH2 at sunset. Chorusing however, which exhibits higher SPLs than RH2 and RH1 (Appeldoorn-Sanders et al. 2023) was detected, but can be heard much further away than RH1. This begs the question whether chorusing is the ultimate long-range call associated with spawning rushes, similarly to the camouflage grouper who produces a boom just before ascent of the spawning rush (Jublier et al. 2019)

The fact that RH1 CAS peaks are no longer occurring at the sunset hours brings us to our second factor. Our results confirmed that chorusing is mostly produced by the symphony of RH1 CAS, as evidenced by the drop in RH2 when RH1 calls peak. However, the fact that chorusing is present with low levels of RH1 at the recorder site in the 2018–2020 period, suggests that chorusing may be happening further than 100 m away from the recorder. Nemeth et al. (2007) observed that at spatial scales of <1 km, red hind showed daily fluctuations of sex ratios around the full moon most likely associated with reproductive activity of females and males during a spawning aggregation. Trap catch data from St. Croix, USVI showed that females occupied outlying areas while males preceded to the aggregation site apparently to establish territories (Colin et al. 1987). Four and three DBFM, trap catches were dominated by males in an area of reef 50–200 m west of the spawning site. One hundred and fifty meters east and west of this male-dominated area, trap catches were mostly females, while in between, catches were composed of equal proportions of males and females. These observations suggest that the calls detected at the location of the hydrophone relative to the fish male/female distribution could be biased by the type of activity (e.g. courtship or territorial/harem defense, or staging) occurring near the hydrophone and within a 100 m radius. The hydrophone could be in a male or female dominated area, a few hundreds of meters away from the spawning site as shown in Fig. 8 of Nemeth et al. (2007). Therefore, the presence of RH1 peaks at hours other than sunset, associated with a decrease in RH2, as seen in the 2013–2017 period could be indicative of courtship activity outside the nucleus of the aggregation area and associated with the daily movement of both males and females. This would imply that starting in 2018, the spawning site is no longer near the current location of the ALS recorder, but chorusing, which is 10 dB louder than ambient sounds can still be captured by the recorder. RH1 CAS, however, could not be as detectable unlike RH2 in a male dominated area, for example.

If it is true that the spawning site within the aggregation area has changed, it thus begs the question as to why. Reproductive phenology is one of the key characteristics of fish populations that may be affected by climate change due to shifts in temperature regimes. For example, modeling the impacts of oceanographic variables on red hind phenology suggested a potential delay in their spawning season over decadal time scales and identified eddy kinetic energy as an important variable (Gokturk et al. 2022). Several studies have suggested that spawning occurs in areas or at times with slower currents that may results in greater probability of self-recruitment (Nemeth et al. 2007, 2008, Kadison et al. 2009, Appeldoorn et al. 2019). Slow currents are the result of a balance between tide driven flows and the mesoscale circulation as shown in Chérubin et al. (2011). Therefore, any change in the mesoscale circulation can affect that balance, hence forcing the fish to find a more suitable location for spawning and gamete release to occur. The latter could be explained by changes in the circulation associated with the mean circulation of the Caribbean Sea and subtropical gyre, which seems to undergo a weakening of its circulation (Jury 2020).

The analysis of the CAS cycles over a 12-year period has confirmed patterns related to celestial cycles that confer predictability to this species' CAS production. The analysis has also revealed the relative temporal variation in CAS type production, which is revealing of their respective roles, behaviors and social structure within the FSA, as suggested by Appeldoorn et al. (2019) and confirmed by Zayas-Santiago et al. (2020) in captivity and in the wild. The timing in increased production of RH1 over RH2 operates as an indicator for timing of spawning-related activity at the FSA, allowing fisheries managers to potentially predict reproduction events via real-time acoustic monitoring. This contribution to the description of red hind ecology further offers means for identifying shifting baselines or changes in the behavior via long-term monitoring effort. The increase in RH2 CAS numbers over the years and in the number of peak calling periods, all associated with chorusing, would suggest a significant change in the red hind population, such as an increase in older males over time and a potential shift of the spawning site, both of which remain to be verified. However, the findings of this study, suggest expanding visual and acoustic monitoring beyond the current FSA recording location to confirm such changes.

Conclusion

Analyzing this large dataset was made possible with the automatic classifier FADAR, which enabled the enumeration of both red hind CAS types RH1 and RH2 in <1 month for the 12-year dataset. As shown in Ibrahim et al. (2024), FADAR is a powerful and effective classifier with high accuracy that also enables the user to quantify FADAR's accuracy on its dataset. Without such classification tool, the analysis of the acoustic data would have taken several years, which is a significant limitation on the usability of long-term acoustic monitoring data in fisheries management.

The presumptive spatiotemporal predictability of FSAs and use of CAS by aggregating species has resulted in the consideration of PAM as an efficient, cost-effective tool to collect data on aggregating populations of soniferous fishes. The hypothesis that CAS detection rates generally scale with population density prompted several recent studies to investigate how accurately such rates can be used to infer fish stock size (Rowell et al. 2012, 2017, Schärer et al., 2012, Sanchez et al., 2017, Caiger et al., 2020, Looby et al., 2022). Despite these efforts, challenges persist. By using an array of hydrophones and monitoring the location of aggregating fishes in relation to these hydrophones across time, van Horn et al. (2025) were able to partition the competing effects of time, space and behaviors on CAS detection rates.

We showed in this study that the relative variation of call types, associated with reproductive behaviors can help distinguish periods of protracted courtship without spawning, if we assume that choruses are indicative of imminent spawning. Because of the key association of the relative RH1 to RH2 CAS ratios to chorusing and potential spawning, the absence of such patterns is most likely indicative of a change in the spawning site and the spatiotemporal dynamics of the red hind FSA, rather than a change in sex-ratios of the spawning population, which is also a possibility. Thus, this understanding enables the use of a single hydrophone to assess population changes and potential spatial shift of the spawning location, although a hydrophone array would provide a more comprehensive view of the aggregation dynamics (van Horn et al. 2025). Therefore, understanding the relative role of call types and monitoring the relative variations of call type numbers in the reproductive dynamics of socially structured populations enables the understanding of potential changes in a spawning aggregation over time as Gokturk et al. (2022) suggested in response to future climate scenarios. Understanding the mating system and reproductive behaviors of aggregating fish are essential for the establishment of effective restoration and management strategies (Grüss et al. 2014, Sadovy de Mitcheson 2016, Erisman et al. 2017). Calling activity and calls' temporal features can be used to inform about fish reproductive condition and spawning in cultured Sciaenidae species (Bolgan et al. 2020). With interpretation of acoustic behavior to extract knowledge of the spatio-temporal patterns of spawning (van Horn et al., 2024, Rowell et al. 2019), changes in population structure, in phenology and in the location of the spawning site can be estimated. The assessment of these changes can be used to assess their driving factors, whether related to environmental, biological or anthropogenic stressors associated with fishing pressure for example (Sala et al. 2001, Sadovy de Mitcheson et al. 2013). Areal and temporal regulations can be designed and implemented to protect spawning aggregations as means to restore reproductive stocks and regional populations (Nemeth 2005, Heppell et al. 2012, Rowell et al. 2019).

However, many of the hypotheses proposed in this study remain to be validated with an understanding of the short-term movements of the red hind male and female cohorts at ALS.

Acknowledgments

Passive acoustic data were collected with the aid of the University of Puerto Rico, Mayagüez campus, the Caribbean Fishery Management Council funding for research, the Caribbean SEAMAP program, and permits provided by the Department of Natural and Environmental Resources (#2014-IC-040). We thank the crew of Orca Too, as well as the volunteer divers and students, primarily Tim Rowell, Kimberly Clouse, and Carlos Zayas, who contributed to the collection of acoustic data. We also express our gratitude to the two reviewers whose insightful comments have improved the quality of this paper.

Author contributions

Laurent. M. Chérubin (Conceptualization [lead], Funding acquisition [lead], Project administration [lead], Resources [lead], Supervision [lead], Writing – original draft [lead]), Caroline Woodward (Formal Analysis [lead], Investigation [lead], Methodology [equal], Software [lead], Visualization [supporting]), Michelle Schärer-Umpierre (Conceptualization [supporting], Data curation [lead], Supervision [supporting], Validation [equal], Writing – review & editing [equal]), Richard Nemeth (Data curation [supporting], Writing – review & editing [equal]), Eric Appeldoorn-Sanders (Writing – review & editing [equal]), Evan Tuohy (Writing – review & editing [supporting]), Richard Appeldoorn (Writing – review & editing [equal]), ali ibrahim (Formal Analysis [supporting], Methodology [supporting]).

Supplementary data

Supplementary data is available at *ICESJMS* online.

Conflict of interest: The authors have no conflicts of interest to declare.

Data availability

The data underlying this article will be shared on reasonable request to the corresponding author.

References

Aalbers SA, Sepulveda CA. The utility of a long-term acoustic recording system for detecting white seabass Atractoscion nobilis spawning sounds. *J Fish Biol.* 2012;**81**:1859–70. https://doi.org/10.1111/j.1095-8649.2012.03399.x

Appeldoorn E, Zayas C, Schärer M *et al.* Temporal patterns among multiple courtship associated sounds in the red hind *Epinephelus guttatus* indicate two spawning aggregations during a single lunar cycle. *Proc Gulf Caribb Fish Inst* 2019;**71**:218–20.

Appeldoorn RS, Rowell TJ, Schärer-Umpierre M *et al.* Corroborating fishermen's knowledge of red hind spawning aggregation sites using passive acoustic mapping techniques. *Proc Gulf Caribb Fish Inst* 2014;**66**:375–8.

Appeldoorn RS, Schärer-Umpierre M, Clouse K *et al.* Spatio-temporal patterns of red hind, *Epinephelus guttatus*, spawning aggregations off the west coast of Puerto Rico: evidence from monitoring courtship associated sounds. *Proc Gulf Caribb Fish Inst* 2016;**68**:92–4.

Appeldoorn RS, Schärer-Umpierre MT, Rowell TJ *et al.* Measuring relative density of spawning Red Hind (*Epinephelus guttatus*) from sound production: consistency within and among sites. *Proc Gulf Caribb Fish Inst* 2013;**65**:281–6.

Appeldoorn-Sanders E, Zayas-Santiago C, Schärer-Umpierre MT. Characterization and temporal patterns of red hind grouper, *Epinephelus guttatus*, choruses at a single aggregation site over a 10-year period. *Environ Biol Fishes* 2023;**106**:1953–69. https://doi.org/10.1007/s10641-023-01476-0

Bolgan M, Crucianelli A, Mylonas CC *et al.* Calling activity and calls' temporal features inform about fish reproductive condition and spawning in three cultured Sciaenidae species. *Aquaculture* 2020;**524**:735243. https://doi.org/10.1016/j.aquaculture.2020.735243

Chérubin LM, Dalgleish F, Ibrahim AK *et al.* Fish spawning aggregations dynamics as inferred from a novel, persistent presence robotic approach. *Front Marine Sci* 2020;**6**:779. https://doi.org/10.3389/fmars.2019.00779

Coleman FC, Koenig CC, Collins LA. Reproductive styles of shallow-water grouper (Pisces: serranidae) in the eastern Gulf of Mexico and the consequences of fishing spawning aggregations. *Environ Biol Fishes* 1996;**47**:129–41. https://doi.org/10.1007/BF00005035

Colin PL, Shapiro DY, Weiler D. Aspects of the reproduction of two groupers, *Epinephelus guttatus* and *E. striatus* in West Indies. *Bul Mar Sci* 1987;**40**:220–30.

Di Iorio L, Bonhomme P, Michez N *et al.* Spatio-temporal surveys of the brown meagre *Sciaena umbra* using passive acoustics for management and conservation. *Biorxiv* 2020:2020–06.

Domeier ML, Colin PL. Tropical reef fish spawning aggregations: defined and reviewed. *Bul Mar Sci* 1997;**60**:698–726.

Erisman B, Heyman W, Kobara S *et al.* Fish spawning aggregations: where well-placed management actions can yield big benefits for fisheries and conservation. *Fish Fish* 2017;**18**:128–44. https://doi.org/10.1111/faf.12132

Eristhee NE, Kadison EL, Murray PA *et al.* Preliminary investigations into the red hind fishery in the British Virgin Islands. *Proc Gulf Caribb Fish Inst* 2006;**57**:374–84.

Gokturk E, Bartlett B, Erisman B *et al.* Loss of suitable ocean habitat and phenological shifts among grouper and snapper spawning aggregations in the Greater Caribbean under climate change. *Mar Ecol Prog Ser* 2022;**699**:91–115, https://doi.org/10.3354/meps14165

Grüss A, Robinson J, Heppell SS *et al.* Conservation and fisheries effects of spawning aggregation marine protected areas: what we know, where we should go and what we need to get there. *ICES J Mar Sci* 2014;**71**:1515–34.

Heppell SA, Semmens BX, Archer SK *et al.* Documenting recovery of a spawning aggregation through size frequency analysis from underwater laser calipers measurements. *Biol Conserv* 2012;**155**:119–27. https://doi.org/10.1016/j.biocon.2012.06.002

Heppell SA, Semmens BX, Semmens CP *et al.* Behavior, hyperstability, and population declines of an aggregating marine fish. *Proc Gulf Caribb Fish Inst* 2014;**66**:379–80.

Ibrahim AK, Zhuang H, Chérubin LM *et al.* An approach for automatic classification of grouper vocalizations with passive acoustic monitoring. *J Acoust Soc Am* 2018;**143**:666–76. https://doi.org/10.1121/1.5022281

Ibrahim AK, Zhuang H, Chérubin LM *et al.* Classification of red hind grouper call types using random ensemble of stacked autoencoders. *J Acoust Soc Am* 2019;**146**:2155. https://doi.org/10.1121/1.5126861

Jones DL. *Fathom Toolbox for MATLAB: Software for Multivariate Ecological and Oceanographic Data Analysis*. St. Petersburg, FL: College of Marine Science, University of South Florida, 2017

Jublier N, Bertucci F, Kever L *et al.* Passive acoustic monitoring reveals diverse fish sound production patterns and the sound of the camouflage grouper, *Epinephelus polyphekadion*, at a spawning aggregation site in Fakarava atoll (French Polynesia). *Aquat Conserv: Marine Freshw Ecosyst* 2020;**30**:42–52, . https://doi.org/10.1002/aqc.3242

Jury MR. Slowing of Caribbean through-flow. *Deep Sea Res Part II* 2020;**180**,104682. https://doi.org/10.1016/j.dsr2.2019.104682

Kadison E, Nemeth RS, Blondeau JE. Investigation of a red hind (*Epinephelus guttatus*) spawning aggregation on Saba Bank in Netherlands Antilles. *Bull Mar Sci* 2009;**85**:101–18.

Lowerre-Barbieri SK, Barbieri RL, Flanders JR *et al.* Use of passive acoustics to determine red drum spawning in Georgia waters. *Trans Am Fish Soc* 2008;**137**:562–75, https://doi.org/10.1577/T04-226.1

Luczkovich JJ, Pullinger RC, Johnson SE *et al.* Identifying the critical spawning habitats of sciaenids using passive acoustics. *Trans Am Fish Soc* 2008; **137**:576–605. https://doi.org/10.1577/T05-290.1

Mann D, Locascio J, Schärer M *et al.* Sounds production by red hind *Epinephelus guttatus* in spatially segregated spawning aggregations. *Aquatic Biol* 2010;**10**:149–54https://doi.org/10.3354/ab00272

Matos-Caballo D. Portrait of the commercial fishery of the red hind, *Epinephelus guttatus*, in Puerto Rico during 1992-1999. *Proc Gulf Caribb Fish Inst* 2002;**53**:446–59.

Munro J, Blok L. The status of stock of groupers and hinds in the Northeastern Caribbean. *Proc Gulf Caribb Fish Inst* 2005;**56**:284–94

Nemeth RS. Population characteristics of a recovering US Virgin Islands red hind spawning aggregation following protection. *Marine Ecol Progr Ser* 2005;**286**:81–97https://doi.org/10.3354/meps286081

Nemeth RS. Chapter 4: dynamics of reef fish and decapod crustacean spawning aggregations: underlying mechanisms, habitat linkages and trophic interactions. In: I Nagelkerken (ed) *Ecological Connectivity Among Tropical Coastal Ecosystems*. Dordrecht: Springer, 2009, 73–134. https://doi.org/10.1007/978-90-481-2406-0

Nemeth RS. Species case studies: red hind—*Epinephelus guttatus*. Chapter 12.3. In Y. Sadovy, P. Colin (eds), *Reef Fish Spawning Aggregations: Biology, Research and Management*, Springer, 2012, 412–7

Nemeth RS, Blondeau J, Herzlieb S *et al.* Spatial and temporal patterns of movement and migration at spawning aggregations of red hind, *Epinephelus guttatus*, in the U.S. Virgin Islands. *Environ Biol Fishes* 2007;**78**:365–81. https://doi.org/10.1007/s10641-006-9161-x

Nemeth RS, Herzlieb S, Blondeau J. Comparison of two seasonal closures for protecting red hind spawning aggregations in the US Virgin Islands. In: *10th International Coral Reef Conference*, Okinawa, Japan, 2006, vol. **4**, pp. 1306–13.

Nemeth RS, Kadison E, Blondeau JE *et al.* Regional coupling of red hind spawning aggregations to oceanographic processes in the eastern Caribbean. *Proc Gulf Caribb Fish Inst* 2008;**59**:170–83.

Parmentier E, Di Iorio L, Picciulin M *et al.* Consistency of spatiotemporal sound features supports the use of passive acoustics for long-term monitoring. *Animal Conserv* 2018;**21**:211–20. https://doi.org/10.1111/acv.12362

Rountree RA, Gilmore RG, Goudey CA *et al.* Listening to fish: applications of passive acoustics to fisheries science. *Fisheries* 2006;**31**:433–46. https://doi.org/10.1577/1548-8446(2006)31%5b433:LTF%5d2.0.CO;2

Rowe S, Hutchings JA. Sound production by atlantic cod during spawning. *Trans Am Fish Soc* 2006;**135**:529–38. https://doi.org/10.1577/T04-061.1

Rowell TJ, Aburto-Oropeza O, Cota-Nieto JJ *et al.* Reproductive behaviour and concurrent sound production of Gulf grouper *Mycteroperca jordani* (Epinephelidae) at a spawning aggregation site. *J Fish Biol*. 2019;**94**:277–96. https://doi.org/10.1111/jfb.13888

Rowell TJ, Appeldoorn RS, Rivera AJ *et al.* Use of passive acoustics to map grouper spawning aggregations, with emphasis on red hind, *Epinephelus guttatus*, off western Puerto Rico. *Proc Gulf Caribb Fish Inst* 2010;**63**:139–42.

Rowell TJ, Nemeth RS, Schärer MT *et al.* Fish sound production and acoustic telemetry reveal behaviors and spatial patterns associated with spawning aggregations of two Caribbean groupers. *Mar Ecol Progr Ser* 2015;**518**:239–54. https://doi.org/10.3354/meps11060

Rowell TJ, Schärer MT, Appeldoorn RS *et al.* Sound production as an indicator of red hind density at a spawning aggregation. *Mar Ecol Progr Ser* 2012;**462**:241–50https://doi.org/10.3354/meps09839

Sadovy Y. Grouper stocks of the western central Atlantic: the need for management and management needs. *Proc Gulf Caribb Fish Inst* 1994;**43**:43–64

Sadovy Y. Reproduction of reef fishery species. In: NVC Polunin, C M Roberts (eds). *Reef Fisheries . Chapman & Hall. Fish and Fisheries Series*, 1996;**20**:15–59. Dordrecht: Springer.

Sadovy Y, Rosario A, Roman A. Reproduction in an aggregating grouper, the red hind, *Epinephelus guttatus*. *Environ Biol Fishes* 1994;**41**:269–86https://doi.org/10.1007/BF02197849

Sadovy de Mitcheson Y, Craig MT, Bertoncini AA *et al.* Fishing groupers towards extinction: a global assessment of threats and extinction risks in a billion dollar fishery. *Fish Fish* 2013;**14**:119–36. https://doi.org/10.1111/j.1467-2979.2011.00455.x

Sadovy de Mitcheson YS. Mainstreaming fish spawning aggregations into fishery management calls for a precautionary approach. *Bioscience* 2016;**66**:295–306. https://doi.org/10.1093/biosci/biw013

Sala E, Ballesteros E, Starr RM., Rapid decline of Nassau grouper spawning aggregations in Belize: fishery management and conservation needs. *Fisheries* 2001;**26**:23–30. https://doi.org/10.1577/1548-8446(2001)026%3c0023:RDONGS%3e2.0.CO;2

Schärer MT, Rowell TJ, Nemeth MI *et al.* Sound production associated with reproductive behavior of Nassau grouper *Epinephelus striatus* at spawning aggregations. *Endanger Species Res* 2012;**19**:29–38. https://doi.org/10.3354/esr00457

Shapiro DY, Sadovy Y, McGehee MA. Size, composition, and spatial structure of the annual spawning aggregation of the red hind, *Epinephelus guttatus* (Pisces: serranidae). *Copeia*, 1993;**1993**:399–406https://doi.org/10.2307/1447138

Stratoudakis Y, Vieira M, Marques JP *et al.* Long-term passive acoustic monitoring to support adaptive management in a sciaenid fishery (Tagus Estuary, Portugal). *Rev Fish Biol Fish* 2024;**34**:491–510. https://doi.org/10.1007/s11160-023-09825-z

Van Horn CJ, Ibrahim AK, Candelmo A *et al.* Hydrophone placement yields high variability in detection of *Epinephelus striatus* calls at a spawning site. *Ecol Appl* 2025; In press.

Walters S, Lowerre-Barbieri S, Bickford J *et al.* Using a passive acoustic survey to identify spotted seatrout spawning sites and associated habitat in Tampa Bay, Florida. *Trans Am Fish Soc* 2009;**138**:88–98. https://doi.org/10.1577/to7-106.1

Whiteman EA, Jennings CA, Nemeth RS. Sex structure and potential female fecundity in a *Epinephelus guttatus* spawning aggregation: applying ultrasonic imaging. *J Fish Biol* 2005; **66**:983–95. https://doi.org/10.1111/j.0022-1112.2005.00653.x

Wilson KC, Semmens BX, Gittings SR *et al.* Grouper source levels and aggregation dynamics inferred from passive acoustic localization at a multispecies spawning site. *J Acoust Soc Am* 2022;**151**:3052–65. https://doi.org/10.1121/10.0010236

Wilson KC, Semmens BX, Pattengill-Semmens CV *et al.* Potential for grouper acoustic competition and partitioning at a multispecies spawning site off Little Cayman, Cayman Islands. *Marine Ecol Progr Ser* 2020;**634**:127–46. https://doi.org/10.3354/meps13181

Woodward C, Schärer-Umpierre M, Nemeth RS *et al.* Spatial distribution of spawning groupers on a Caribbean reef from an autonomous surface platform. *Fish Res* 2023;**266**:106794, https://doi.org/10.1016/j.fishres.2023.106794

Zayas-Santiago CM, Appeldoorn R, Schärer-Umpierre MT *et al.* Red hind *Epinephelus guttatus* vocal repertoire characterization, behavior, and temporal patterns. *Gulf Caribbean Res* 2020;**31**:GCFI31–41. https://doi.org/10.18785/gcr.3101.17

Handling editor: Francis Juanes